Title	Characterization of a thermostable 2,4-diaminopentanoate dehydrogenase from Fervidobacterium nodosum Rt17-B1.
Author(s)	Fukuyama, Sadanobu; Mihara, Hisaaki; Miyake, Ryoma; Ueda, Makoto; Esaki, Nobuyoshi; Kurihara, Tatsuo
Citation	Journal of bioscience and bioengineering (2014), 117(5): 551-556
Issue Date	2014-05
URL	http://hdl.handle.net/2433/187042
Right	© 2013 The Society for Biotechnology, Japan. Published by Elsevier B.V.
Type	Journal Article
Textversion	author

Characterization of a thermostable 2,4-diaminopentanoate dehydrogenase from *Fervidobacterium nodosum* Rt17-B1

Sadanobu Fukuyama,[1] Hisaaki Mihara,[1] Ryoma Miyake,[2,3] Makoto Ueda,[2,3] Nobuyoshi Esaki,[1] and Tatsuo Kurihara[1,*]

[1]Institute for Chemical Research, Kyoto University, Uji, Kyoto 611-0011, Japan

[2]Mitsubishi Chemical Group Science and Technology Research Center, Inc., Yokohama 227-8502, Japan

[3]API Corporation, Yokohama 227-8502, Japan

*Corresponding author. Tel: +81-774-38-4710, Fax: +81-774-38-3248, E-mail: kurihara@scl.kyoto-u.ac.jp

Present addresses.

S. F.: KOGA ISOTOPE, Ltd., Koka, Shiga 520-3404, Japan

H. M.: Department of Biotechnology, College of Life Sciences, Ritsumeikan University, Kusatsu, Shiga 525-8577, Japan

M. U.: Department of Materials Chemistry and Bioengineering, Oyama National College of Technology, Oyama, Tochigi 323-0806, Japan

Running title: Thermophilic 2,4-diaminopentanoate dehydrogenase

Key words: 2,4-diaminopentanoate dehydrogenase; *Fervidobacterium nodosum*; amino acid dehydrogenase; ornithine metabolism; deamination; amination; thermophilic enzyme

Abstract

2,4-Diaminopentanoate dehydrogenase (2,4-DAPDH), which is involved in the oxidative ornithine degradation pathway, catalyzes the NAD^+- or $NADP^+$-dependent oxidative deamination of (2*R*, 4*S*)-2,4-diaminopentanoate (2,4-DAP) to form 2-amino-4-oxopentanoate. A *Fervidobacterium nodosum* Rt17-B1 gene, *Fnod_1646*, which codes for a protein with sequence similarity to 2,4-DAPDH discovered in metagenomic DNA, was cloned and overexpressed in *Escherichia coli*, and the gene product was purified and characterized. The purified protein catalyzed the reduction of NAD^+ and $NADP^+$ in the presence of 2,4-DAP, indicating that the protein is a 2,4-DAPDH. The optimal pH and temperature were 9.5 and 85°C, respectively, and the half-denaturation time at 90°C was 38 min. Therefore, the 2,4-DAPDH from *F. nodosum* Rt17-B1 is an $NAD(P)^+$-dependent thermophilic-alkaline amino acid dehydrogenase. This is the first thermophilic 2,4-DAPDH reported, and it is expected to be useful for structural and functional analyses of 2,4-DAPDH and for the enzymatic production of chiral amine compounds. Activity of 2,4-DAPDH from *F. nodosum* Rt17-B1 was suppressed by 2,4-DAP via uncompetitive substrate inhibition. In contrast, the enzyme showed typical Michaelis-Menten kinetics toward 2,5-diaminohexanoate. The enzyme was uncompetitively inhibited by D-ornithine with an apparent K_i value of 0.1 mM. These results suggest a regulatory role for this enzyme in the oxidative ornithine degradation pathway.

Introduction

2,4-Diaminopentanoate dehydrogenase (2,4-DAPDH, EC 1.4.1.12) catalyzes NAD^+- or $NADP^+$-dependent oxidative deamination of (2*R*, 4*S*)-2,4-diaminopentanoate (2,4-DAP) at carbon 4 to form 2-amino-4-oxopentanoate (AKP) (1). In the 1970s, this enzyme was first discovered in a crude extract of *Clostridium sticklandii* as a part of the oxidative ornithine degradation pathway (Fig. 1) (2-4), and the genes implicated in this pathway were recently identified through a metagenomics approach in an anaerobic digester from a wastewater treatment plant (5). The oxidative ornithine degradation pathway has also been verified in several anaerobic genera, including *Clostridium*, *Thermoanaerobacter*, *Propionibacterium*, and *Fervidobacterium*. The first step in this pathway is the conversion of L-ornithine to the D isomer by ornithine racemase (6). D-Ornithine is then converted to 2,4-DAP by D-ornithine aminomutase (OAM), an adenosylcobalamine (AdoCbl) and pyridoxal phosphate (PLP)-dependent enzyme, in which the amino group at carbon 5 is migrated to carbon 4 (7). 2,4-DAP is then oxidatively deaminated to form AKP. In the final step in this pathway, AKP undergoes a thiolytic cleavage, which is catalyzed by AKP thiolase with coenzyme A, to form acetyl-CoA and D-alanine (8).

Chiral amines are important starting materials for the synthesis of pharmaceuticals and agrochemicals. To obtain these chiral amine compounds, a variety of chemical and enzymatic methods have been utilized. Some examples include the enzymatic synthesis of chiral amines with lipases (9, 10) and ω-amino acid aminotransferases (11, 12). One drawback of most of these strategies is that they require auxiliary compounds and involve multistep transformations. In addition, in synthesis methods using an aminotransferase, the yield of the product is often unsatisfactory due to the reaction equilibrium. These drawbacks may be overcome by using amino acid dehydrogenases. Amino acid dehydrogenases catalyze the reduction of α-keto acids with concomitant amination of the substrates with NAD(P)H and an ammonium ion. Therefore, these enzymes are useful for producing chiral amines from the corresponding α-keto acid compounds in one step along with an established

NAD(P)H recycling system. The product yield might also be enhanced by increasing the concentration of NAD(P)H with an NAD(P)H regeneration system. However, despite these advantages, the applications for amino acid dehydrogenases have been limited to the production of α-amino acids. 2,4-DAPDH may expand the application range of amino acid dehydrogenases for the production of other chiral amine compounds, because 2,4-DAPDH should catalyze the amination of the carbonyl group at the γ position.

Thermostable enzymes from thermophilic organisms have been used extensively in industry because these enzymes are inherently stable in harsh industrial processes. *Fervidobacterium* belongs to the eubacterial order of *Thermotogales*, which includes the most extremely thermophilic eubacteria presently known. It can grow at temperatures above 60°C with an optimal temperature of approximately 80°C (13). In this study, we carried out gene cloning, overexpression, purification, and biochemical characterization of a thermostable 2,4-DAPDH from the thermophilic anaerobic bacterium, *Fervidobacterium nodosum* Rt17-B1. This is the first report of a thermophilic 2,4-DAPDH. The role of this enzyme in the oxidative ornithine degradation pathway is also discussed.

Materials and Methods

Materials

Restriction enzymes and kits for genetic manipulation were obtained from Takara Bio (Kyoto, Japan), New England Biolabs (Ipswich, MA), and Stratagene (La Jolla, CA). The pET14b expression vector was purchased from Novagen (Madison, WI). His-bind Resin was obtained from Novagen. All other reagents were of analytical grade and were from Nacalai Tesque (Kyoto, Japan) and Wako Pure Chemical Industries (Osaka, Japan).

Cloning of the 2,4-DAPDH gene from F. nodosum Rt17-B1

Genomic DNA was isolated from *F. nodosum* Rt17-B1 (DSMZ, Braunschweig, Germany) using a DNeasy Blood & Tissue Kit (Qiagen, Venlo, Netherlands) according to the manufacturer's instructions. The gene encoding 2,4-DAPDH was amplified by overlap extension PCR to remove the intrinsic NdeI site in the coding region. Two separate amplification reactions were performed using Phusion DNA polymerase (Finnzymes, Espoo, Finland), 100 ng of genomic DNA as a template, and the following two sets of primers: Fnod_1646 NdeI N (5'-GCGGGAATTCCATATGCGTATAGTTACTTGGGG-3') and Fnod_1646 deNdeI R (5'-CATTTATCGCCAACGTATGCTTTTGCTG-3') to amplify the DNA coding for the N-terminal part of the protein, and Fnod_1646 deNdeI F (5'-CAGCAAAAGCATACGTTGGCGATAAATG-3') and Fnod_1646 BamHI C (5'-GCCGCGGATCCTCATTCCATTTGAGAAAGGATTG-3') to amplify the DNA coding for the C-terminal part of the protein. The underlined sequences indicate the restriction sites for NdeI and BamHI, respectively. The double-underlined sequences indicate the sites that anneal to the intrinsic NdeI site in the coding region. The PCR products were mixed and used as templates in a second PCR to amplify the full-length gene using Fnod_1646 NdeI N and Fnod_1646 BamHI C. The amplified product was digested with NdeI and BamHI and inserted into the corresponding sites of pET14b to generate an N-terminal His6-tagged protein. The recombinant

plasmid was designated pET_Fnod_DAPDH.

Expression and purification of 2,4-DAPDH

pET_Fnod_DAPDH was introduced into *Escherichia coli* Rosetta (DE3), and the cells were grown in LB medium containing 0.1 mM IPTG at 28°C for 15–17 h. The cells were harvested by centrifugation, resuspended in 50 mM Tris-HCl (pH 8.0), and homogenized by sonication. The homogenate was centrifuged at 25,000 × *g* for 40 min at 4°C. The supernatant was loaded onto a His-bind column (10 mL) equilibrated with 50 mM Tris-HCl (pH 8.0). The enzyme was eluted with a 600-mL linear gradient of 0–500 mM imidazole in the same buffer. The enzyme fractions were pooled and dialyzed against 50 mM Tris-HCl (pH 8.0). The final preparation of the enzyme was stored at -80°C until use.

Synthesis of 2,4-DAP

2,4-DAP was obtained from D-ornithine by enzymatic synthesis using OAM. To prepare OAM, which is comprised of two subunits, OraS and OraE, the genes coding for these subunits were amplified by PCR from *F. nodosum* genomic DNA using the following two sets of primers: FnodOAMS_N_Bam (5'-GGAGGGGATCCGATGAAACCAAGGCCG-3') and FnodOAMS_C_Hind (5'-TTTTCTTGGGTCGAGTTAAGCTTTTATTTAC-3') for *oraS* and FnodOAME_N_Nde (5'-GCGGTGAGTAACATATGGACAAAC-3') and FnodOAME_C_Xho (5'-GAATTTGACTCGAGTTATTTTTGAGATTC-3') for *oraE*. The underlined sequences indicate the restriction sites for BamHI, HindIII, NdeI, and XhoI, respectively. The *oraS* PCR product was digested with BamHI and HindIII and inserted into the corresponding sites of Multiple cloning site-1 of pCOLA Duet-1, and the *oraE* PCR product was digested with NdeI and XhoI and inserted into the corresponding sites of Multiple cloning site-2 of the same plasmid. The recombinant plasmid was designated pCOLA_Fnod_OAM.

E. coli Rosetta (DE3) cells harboring the expression plasmid pCOLA_Fnod_OAM were grown in LB medium containing 0.1 mM IPTG at 28°C for 15–17 h. The cells were harvested by centrifugation, resuspended in a 25-mM ACES buffer (pH 6.5), and homogenized by sonication. The homogenate containing OAM was used to synthesize 2,4-DAP from D-ornithine.

The reaction mixture for the synthesis of 2,4-DAP consisted of 25 mM ACES buffer (pH 6.5), 50 mM D-ornithine, 50 μM PLP, 50 μM AdoCbl, 1 mM DTT, and the homogenate. The reaction was performed in the dark on a magnetic stirrer plate at 55°C for 21 h. The reaction was terminated by the addition of trichloroacetic acid (final concentration, 25%). After centrifugation and three ether extractions, the extract was evaporated and taken up in water. The solution was desalted with a Dowex-50W-X8, 200 to 400 mesh, H^+-form column. After washing, the D-ornithine and 2,4-DAP adsorbed to the column were eluted with 1 M NH_4OH. The D-ornithine and 2,4-DAP fractions were pooled, evaporated, and reconstituted in chloroform:methanol:15% NH_4OH (36:46:20). D-Ornithine and 2,4-DAP were then separated by column chromatography by using silicic acid (Silica Gel 60, 100 to 210 mesh; KANTO CHEMICAL, Tokyo, Japan) with chloroform:methanol:15% NH_4OH (36: 46: 20). The 2,4-DAP fractions were pooled and evaporated.

Synthesis of 2,5-diaminohexanoate (2,5-DAH)

2,5-DAH was obtained from D-lysine by enzymatic synthesis with lysine 5,6-aminomutase. To obtain the enzyme, which is comprised of two subunits, KamD and KamE, the genes coding for these subunits were amplified from *Thermoanaerobacter tengcongensis* genomic DNA by PCR using the following two sets of primers: TTELAMa_N_Bam (5'-GAGGGGATCCGATGAAGAAGAGCAAG-3') and TTELAMa_C_Sal (5'-GGCGTCGACTCATCCTCTATCACCTCTT-3') for *kamD* and TTELAMb_N_Nde (5'-GGTGATAGCATATGAACAGCGG-3') and TTELAMb_C_Xho (5'-AATCGGCTCGAGTTATTTTTTATACCCTT-3') for *kamE*. The underlined sequences indicate

the restriction sites for BamHI, SalI, NdeI, and XhoI, respectively. The *kamD* PCR product was digested with BamHI and SalI and inserted into the corresponding sites in Multiple cloning site-1 of pCOLA Duet-1. The *kamE* PCR product was digested with NdeI and XhoI and inserted into the corresponding sites in Multiple cloning site-2 of the same plasmid. The recombinant plasmid was designated pCOLA_TTE_LAM.

E. coli Rosetta (DE3) cells harboring the expression plasmid pCOLA_TTE_LAM were grown in LB medium containing 0.1 mM IPTG at 28°C for 15–17 h. The cells were harvested by centrifugation, suspended in 25 mM PIPES buffer (pH 6.5), and homogenized by sonication. The homogenate containing lysine 5,6-aminomutase was used to synthesize 2,5-DAH from D-lysine.

The reaction mixture for the synthesis of 2,5-DAH consisted of 25 mM PIPES buffer (pH6.5), 50 mM D-lysine, 50 μM PLP, 50 μM AdoCbl, 1 mM DTT, and the homogenate. The reaction was performed in the dark on a magnetic stirrer plate at 55°C for 21 h. The reaction was terminated by the addition of trichloroacetic acid (final concentration, 25%). After centrifugation and three ether extractions, the supernatant was concentrated by evaporation and taken up in water. The solution was desalted by using a Dowex-50W-X8, 200 to 400 mesh, H^+-form column. After washing, the D-lysine and 2,5-DAH adsorbed to the column were eluted with 1 M NH_4OH. The D-lysine and 2,5-DAH fractions were pooled, evaporated, and reconstituted in chloroform:methanol:15% NH_4OH (6:70:20). D-Lysine and 2,5-DAH were then separated by column chromatography using silicic acid (Silica Gel 60, 100 to 210 mesh; KANTO CHEMICAL) with chloroform:methanol:15% NH_4OH (6:70:20). The 2,5-DAH fractions were pooled and evaporated.

Enzyme assay

The activity of 2,4-DAPDH was determined spectrophotometrically by monitoring the change in A_{340} upon the reduction of NAD^+ at 55°C. The assay mixture consisted of 0.5 mM NAD^+, 0.5 mM substrate, and 50 mM HEPES-NaOH (pH 8.5). The reaction was started by the addition of the

187 enzyme.

188

189 *Determination of optimal pH and temperature*

190 The pH optimum of the enzyme was determined using the following four buffer systems: 50
191 mM acetate buffer (pH 5–5.5), 50 mM potassium phosphate buffer (KPB) (pH 5.5–7), HEPES-NaOH
192 buffer (pH 7–8.5), and CHES-NaOH buffer (pH 8.5–10). The optimal temperature of the enzyme was
193 determined by measuring the enzyme activity over the temperature range of 5°C–95°C.

194

195 *Determination of thermostability*

196 The stability of the 2,4-DAPDH enzyme at elevated temperatures was investigated by
197 incubating the enzyme in 50 mM HEPES-NaOH (pH 8.5) at 90°C and 100°C. At certain time intervals,
198 samples were withdrawn, and the residual activity was measured under standard assay conditions.

199

200 *Effect of metal ions and reagents*

201 The effects of metal ions and various reagents on the enzyme were determined by measuring
202 activity after incubating it in 50 mM HEPES-NaOH (pH 8.5) with and without different metal ions and
203 reagents at 0.5 mM.

204

205 *Determination of kinetic parameters*

206 The initial rates of the enzyme reaction were measured while varying the concentration of
207 one substrate while the concentration of the other substrate was held constant (and in excess). Data
208 were fitted to the Michaelis-Menten equation, and the kinetic parameters were calculated using
209 nonlinear least-squares regression with Kaleida Graph software (Adelbeck Software, Reading, PA).
210 Substrate inhibition studies were performed with various concentrations of 2,4-DAP and a fixed
211 saturating concentration of NAD^+ (0.5 mM). The data were fitted to Equation 1, which is the standard

212 equation for complete uncompetitive substrate inhibition.

213 $v = V_{max}/\{1 + (K/[S]) + ([S]/K_i)\}$ (Equation 1)

214 In Equation 1, v and V_{max} are the initial and maximum velocities, respectively, [S] is the substrate
215 concentration, K is Michaelis constant for the substrate, and K_i is the inhibition constant for the
216 substrate.

217 Inhibitor studies of 2,4-DAPDH employed the assay described above. The kinetic analysis
218 was conducted with various concentrations of 2,4-DAP (0.01, 0.025, 0.05, 0.1, and 0.2 mM) and
219 D-ornithine (0.5, 1.5, and 2.0 mM). The K_i value was calculated from the Dixon plot.

220

221

Results

Identification and characterization of 2,4-DAPDH from F. nodosum Rt17-B1

To obtain a 2,4-DAPDH with superior thermostability, we focused on the thermophilic bacterium *F. nodosum* Rt17-B1. This strain was believed to have a functional oxidative degradation pathway for ornithine because it has *oraS* and *oraE* homologues that encode the S and E subunits of ornithine aminomutase, respectively. In the genome sequence of *F. nodosum*, the candidate gene for 2,4-DAPDH, *Fnod_1646* (GenBank accession number: ABS61481.1), is adjacent to the *oraS* and *oraE* homologues. The putative protein encoded by *Fnod_1646* is a homologue of the 2,4-DAPDH found in a metagenome from an anaerobic digester at a waste water-treatment plant (58.0% identity), which has been described as a homodimer with a subunit molecular mass of approximately 36 kDa that catalyzes the NAD^+-dependent oxidation of 2,4-DAP to AKP. The protein encoded by *Fnod_1646* has a predicted molecular mass of 38 kDa and the GXGXXG sequence motif characteristic of the Rossmann fold, which is a typical of $NAD(P)^+$-binding proteins.

To examine the enzyme activity of this protein, the *Fnod_1646* gene was cloned into the pET14b expression plasmid to construct pET_Fnod_DAPDH, and then heterologously expressed under the control of the T7 promoter in *E. coli* Rosetta (DE3) as an N-terminal His-tagged fusion. The gene product was purified in a single step by Ni-affinity chromatography. The homogeneity of the purified protein was verified by SDS-PAGE, which showed a single band with an apparent molecular mass of 38 kDa. In a reaction mixture containing 2,4-DAP, the purified protein catalyzed the reduction of NAD^+ to NADH, indicating that the protein is a 2,4-DAPDH.

Optimal pH and thermostability

To determine the optimal pH for 2,4-DAPDH, the activity of the enzyme was measured at 55°C using 2,4-DAP as a substrate at pH 5.0–10. It showed maximum activity at pH 9.5 and high activity (>70% of maximum activity) at alkaline pHs in the range of 9.0–10.0 (Fig. 2). Enzymatic

247 activity was routinely determined at pH 8.5 (HEPES-NaOH buffer) in this study because NAD^+ is
248 unstable at pH 9.0–10.0.

249 To determine the effect of temperature on enzyme activity, reactions were conducted using
250 2,4-DAP as a substrate in 50 mM HEPES-NaOH buffer (pH 8.5) over a temperature range of
251 5°C–95°C. The enzyme showed maximum activity at 85°C (Fig. 3). To test the thermostability of
252 2,4-DAPDH, the enzyme was incubated at 90°C and 100°C, and the residual activity was assayed. The
253 half-life of the enzyme was estimated to be 38 min at 90°C and 2 min at 100°C (data not shown).

254

255 *Effect of various reagents on 2,4-DAPDH activity*

256 2,4-DAPDH activity was measured in the presence of EDTA and various divalent metal ions
257 at a concentration of 0.5 mM (Table 1). EDTA did not affect 2,4-DAPDH activity. Mn^{2+} had no
258 significant effect on 2,4-DAPDH activity, whereas Mg^{2+}, Ca^{2+}, Fe^{2+}, and Co^{2+} moderately inhibited the
259 activity, and Ni^{2+}, Cu^{2+}, and Zn^{2+} almost completely inhibited the activity. Adding EDTA to the
260 reaction mixture at a concentration equal to that of the metal ion completely suppressed the inhibition,
261 indicating that these metals reversibly inactivated the enzyme (data not shown). K^+ and anions of the
262 salts shown in Table 1 did not affect enzyme activity.

263

264 *Coenzyme and substrate specificity*

265 The coenzyme specificity of 2,4-DAPDH was examined by measuring enzyme activity
266 using 2,4-DAP as a substrate and either NAD^+ or $NADP^+$ as the coenzyme. The experiment showed
267 that the enzyme uses both NAD^+ and $NADP^+$ as a coenzyme (92 and 17 $\mu mol \cdot min^{-1} \cdot mg^{-1}$, respectively).
268 However, the activity of the enzyme with NAD^+ was 5.4 times higher than that with $NADP^+$. Therefore,
269 the enzyme prefers to use NAD^+ as a coenzyme.

270 The substrate specificity of the enzyme during NAD^+-dependent oxidative deamination was
271 examined using 0.5 mM 2,4-DAP or 2,5-DAH. 2,5-DAH is produced by lysine 5,6-aminomutase,

which catalyzes the 5,6-rearrangement of the terminal amino group of D-lysine in the lysine degradation pathway (Fig. 1). 2,4-DAPDH from *F. nodosum* acted not only on 2,4-DAP (92 $\mu mol \cdot min^{-1} \cdot mg^{-1}$) but also on 2,5-DAH (1 $\mu mol \cdot min^{-1} \cdot mg^{-1}$). The activity of the enzyme using 2,4-DAP as a substrate was approximately 90 times higher than that using 2,5-DAH.

Kinetic parameters of 2,4-DAPDH

Kinetic analysis of the enzyme was performed using 0.005–1 mM NAD^+ or 0.1–8 mM $NADP^+$ as a coenzyme. The kinetic parameters determined are shown in Table 2. The K_m value for NAD^+ was about 40 times lower than that for $NADP^+$, whereas the V_{max} and k_{cat} values for NAD^+ and $NADP^+$ were similar.

The activities of the enzyme were measured at various concentrations of 2,4-DAP and 2,5-DAH. The enzyme displayed non-Michaelis-Menten kinetics with 2,4-DAP as the substrate. Although the enzymatic activity increased as the 2,4-DAP concentration increased over the range of 0–0.8 mM, it decreased at 2,4-DAP concentrations over 0.8 mM (Fig. 4). This behavior is consistent with complete uncompetitive substrate inhibition, and the experimental data are fitted well by the equation describing this type of inhibition (Equation 1 in the Materials and Methods). An apparent K_i value and K_m value were calculated as 0.9 mM and 0.2 mM, respectively (Table 2). In contrast, the enzyme displayed typical Michaelis-Menten kinetics when 2,5-DAH (0–10 mM) was used as the substrate (Fig. 5). The kinetic parameters for these substrates are summarized in Table 2.

Regulation of 2,4-DAPDH

We examined whether the activity of 2,4-DAPDH is affected by D-ornithine and D-alanine, which occur as metabolites in the oxidative ornithine degradation pathway (Fig. 1). Enzyme activity was measured in a solution of 50 mM HEPES pH 8.5, 1 mM NAD^+, and 0.3 mM 2,4-DAP in the presence or absence of these amino acids. Enzymatic activity decreased to 14% and 71% of the

297 positive control in the presence of 5 mM D-ornithine and D-alanine, respectively. We also examined
298 whether D-lysine affects enzyme activity under these same conditions. The activity decreased to 68%
299 of the positive control following the addition of 5 mM D-lysine. Therefore, the activity of 2,4-DAPDH
300 is suppressed in the presence of D-ornithine, D-alanine, and D-lysine. D-Ornithine is the most effective
301 inhibitor. To further characterize the inhibition by D-ornithine, enzyme activity toward 2,4-DAPDH
302 was measured in the presence of varying concentrations of D-ornithine. In double-reciprocal plots of
303 enzyme activity versus 2,4-DAP concentration, a set of parallel linear lines were obtained (Fig. 6),
304 indicating that D-ornithine acts as an uncompetitive inhibitor of 2,4-DAPDH. The apparent K_i value
305 was 0.1 mM.
306
307

Discussion

In this paper, the gene cloning, expression, and characterization of a thermostable 2,4-DAPDH from the thermophilic bacterium *F. nodosum* Rt17-B1 are described. The gene from this bacterium, *Fnod_1646*, was predicted to encode a 2,4-DAPDH. The protein, which was purified from recombinant *E. coli* cells, showed a molecular mass of 38 kDa on SDS-PAGE and catalyzed the oxidative deamination of 2,4-DAP in an $NAD(P)^+$-dependent manner. The optimum pH for 2,4-DAP oxidation was in the alkaline range. A variety of metals, such as Cu^{2+}, Ni^{2+}, and Zn^{2+}, inhibited its catalytic activity. This 2,4-DAPDH is noteworthy because it has a high optimal temperature and is thermostable. The optimal temperature for this enzyme in 2,4-DAP oxidation was 85°C. Therefore, the enzyme is an $NAD(P)^+$-dependent thermophilic alkaline amino acid dehydrogenase.

We found that besides 2,4-DAP, 2,5-DAH can also serve as the substrate for 2,4-DAPDH (Table 2). 2,5-DAH may be produced from D-lysine by lysine-5,6-aminomutase (14), raising the possibility that 2,4-DAPDH also participates in lysine degradation (Fig. 1). However, the k_{cat}/K_m value of 2,4-DAPDH for 2,5-DAH is much lower than that for 2,4-DAP, implying that 2,5-DAH is not a physiological substrate of 2,4-DAPDH. The validity of this interpretation should be verified in future *in vivo* studies.

In this study, we found notable regulatory properties of 2,4-DAPDH, including uncompetitive substrate inhibition by 2,4-DAP and uncompetitive inhibition by D-ornithine. These results suggest that the oxidative degradation of ornithine is regulated by upstream metabolites; at high concentrations of D-ornithine and 2,4-DAP, this degradation pathway is suppressed. It is known that substrate inhibition of enzymes, such as tyrosine hydroxylase, plays a role in stabilizing the reaction rate against large fluctuations in substrate concentration (15). Therefore, upstream regulation of the oxidative ornithine degradation pathway may result in a steady synthesis of downstream metabolites, such as the D-alanine that is required for the synthesis of peptidoglycan (16, 17), under conditions at which the concentrations of the upstream metabolites fluctuate.

The regulation of 2,4-DAPDH may also affect the metabolic fate of ornithine, which may be metabolized via four different pathways, as analysis of the *F. nodosum* genome and previous reports suggested the occurrence of four ornithine metabolic pathways in this bacterium. The first is the oxidative degradation pathway that was the focus of this study. The second is a spermidine and spermine biosynthesis pathway, which starts with the conversion of L-ornithine into putrescine by ornithine decarboxylase. Polyamines, such as spermidine and spermine, are polycationic compounds that are implicated in a wide variety of biological reactions, including the synthesis of nucleobases and proteins (20). The third is the urea cycle in which ornithine is metabolized by ornithine carbamoyltransferase (19). The fourth is the reductive degradation pathway in which ornithine is reduced to 5-aminovalerate through the formation of proline (5). This reductive pathway has been found in anaerobic bacteria such as *C. sticklandii* (18). Inhibition of 2,4-DAPDH by the upstream metabolites in the oxidative ornithine degradation pathway may direct the metabolic flux of L-ornithine to other pathways. This should be examined in future studies by *in vivo* experiments.

Amino acid dehydrogenases are useful for the synthesis of chiral amino acids from the corresponding keto acids. Because most amino acid dehydrogenases characterized thus far catalyze the interconversion between α-amino acids and α-keto acids, this method has only been used for the production of chiral α-amino acids. Based on its activity toward 2,4-DAP and 2,5-DAH, 2,4-DAPDH should catalyze the reductive amination of the carbonyl group at the γ-position and the δ-position, which differs from the activity of most previously characterized amino acid dehydrogenases. In a preliminary experiment, we tested the reductive amination of 2,4-DAPDH using the oxidative deamination product of 2,4-DAP. After 2,4-DAP was converted to AKP, the reaction was stopped by heat treatment, and AKP was used as the substrate for reductive amination reaction. 2,4-DAPDH catalyzed the AKP-dependent oxidation of NADH, implying that the enzyme catalyzed the reductive amination of AKP (data not shown). Therefore, 2,4-DAPDH is expected to expand the range of chiral amine compounds (other than α-amino acids) produced by amino acid dehydrogenases. When

considering such applications, the thermostability of the enzyme is beneficial. Possible applications in the synthesis of chiral amine compounds for the thermostable 2,4-DAPDH identified in this study are currently under investigation.

Acknowledgments

This work was supported in part by the Collaborative Research Program of Institute for Chemical Research, Kyoto University (grant # 2013-59).

References

1. **Somack, R. and Costilow, R. N.**: 2,4-Diaminopentanoic acid C_4 dehydrogenase. Purification and properties of the protein, J. Biol. Chem., **248**, 385-388 (1973).

2. **Dyer, J. K. and Costilow, R. N.**: 2,4-Diaminovaleric acid: an intermediate in the anaerobic oxidation of ornithine by *Clostridium sticklandii*, J. Bacteriol., **101**, 77-83 (1970).

3. **Tsuda, Y. and Friedmann, H. C.**: Ornithine metabolism by *Clostridium sticklandii*. Oxidation of ornithine to 2-amino-4-ketopentanoic acid via 2,4-diaminopentanoic acid; participation of B_{12} coenzyme, pyridoxal phosphate, and pyridine nucleotide, J. Biol. Chem., **245**, 5914-5926 (1970).

4. **Barker, H. A.**: Amino acid degradation by anaerobic bacteria, Annu. Rev. Biochem., **50**, 23-40 (1981).

5. **Fonknechten, N., Perret, A., Perchat, N., Tricot, S., Lechaplais, C., Vallenet, D., Vergne, C., Zaparucha, A., Le Paslier, D., Weissenbach, J., and Salanoubat, M.**: A conserved gene cluster rules anaerobic oxidative degradation of L-ornithine, J. Bacteriol., **191**, 3162-3167 (2009).

6. **Chen, H. P., Lin, C. F., Lee, Y. J., Tsay, S. S., and Wu, S. H.**: Purification and properties of ornithine racemase from *Clostridium sticklandii*, J. Bacteriol., **182**, 2052-2054 (2000).

7. **Somack, R. and Costilow, R. N.**: Purification and properties of a pyridoxal phosphate and coenzyme B_{12} dependent D-α-ornithine 5,4-aminomutase, Biochemistry, **12**, 2597-2604 (1973).

8. **Jeng, I. M., Somack, R., and Barker, H. A.**: Ornithine degradation in *Clostridium sticklandii*; pyridoxal phosphate and coenzyme A dependent thiolytic cleavage of 2-amino-4-ketopentanoate to alanine and acetyl coenzyme A, Biochemistry, **13**, 2898-2903 (1974).

9. **Torres-Gavilán, A., Escalante, J., Regla, I., López-Munguía, A., and Castillo, E.**: 'Easy-on, easy-off' resolution of chiral 1-phenylethylamine catalyzed by *Candida antarctica* lipase B, Tetrahedron: Asymmetry, **18**, 2621-2624 (2007).

10. **Pilissão, C., Carvalho, P. O., and Nascimento, M. G.**: Enantioselective acylation of (*RS*)-phenylethylamine catalysed by lipases, Process Biochem., **44**, 1352-1357 (2009).

11. **Koszelewski, D., Tauber, K., Faber, K., and Kroutil, W.**: ω-Transaminases for the synthesis of non-racemic α-chiral primary amines, Trends Biotechnol., **28**, 324-332 (2010).

12. **Tufvesson, P., Lima-Ramos, J., Jensen, J. S., Al-Haque, N., Neto, W., and Woodley, J. M.**: Process considerations for the asymmetric synthesis of chiral amines using transaminases, Biotechnol. Bioeng., **108**, 1479-1493 (2011).

13. **Patel, B. K. C., Morgan, H. W., and Daniel, R. M.**: *Fervidobacterium nodosum* gen. nov. and spec. nov., a new chemoorganotrophic, caldoactive, anaerobic bacterium, Arch. Microbiol., **141**, 63-69 (1985).

14. **Stadtman, T. C.**: Lysine metabolism by Clostridia, Advance in Enzymology and Related Areas of Molecular Biology, **38**, 413-448 (1973).

15. **Reed, M. C., Lieb, A., and Nijhout, H. F.**: The biological significance of substrate inhibition: a mechanism with diverse functions, Bioessays, **32**, 422-429 (2010).

16. **van Heijenoort, J.**: Formation of the glycan chains in the synthesis of bacterial peptidoglycan, Glycobiology, **11**, 25R-36R (2001).

17. **van Heijenoort, J.**: Recent advances in the formation of the bacterial peptidoglycan monomer unit, Nat. Prod. Rep., **18**, 503-519 (2001).

18. **Kenklies, J., Ziehn, R., Fritsche, K., Pich, A., and Andreesen, J. R.**: Proline biosynthesis from L-ornithine in *Clostridium sticklandii*: purification of Δ^1-pyrroline-5-carboxylate reductase, and sequence and expression of the encoding gene, *proC*, Microbiology, **145**, 819-826 (1999).

19. **Legrain, C., Stalon, V., Noullez, J. P., Mercenier, A., Simon, J. P., Broman, K., and Wiame, J. M.**: Structure and function of ornithine carbamoyltransferases, Eur. J. Biochem., **80**, 401-409 (1977).

20. **Tabor, C. W. and Tabor, H.**: Polyamines in microorganisms, Microbiol. Rev., **49**, 81-99

(1985).

420 Figure Legends

421 Figure 1. The ornithine oxidative degradation pathway and putative lysine degradation pathway.
422 Ornithine racemase, D-ornithine 4,5-aminomutase, 2,4-diaminopentanoate dehydrogenase,
423 2-amino-4-ketopentanoate thiolase, lysine racemase, and D-lysine 5,6-aminomutase catalyze reactions
424 1, 2, 3, 4, 5, and 6 respectively. Reaction 7 is non-enzymatic intramolecular cyclization.

425

426 Figure 2. Effect of pH on the activity of the 2,4-DAPDH from the thermophilic anaerobic bacterium, *F.*
427 *nodosum* Rt17-B1. Enzyme assays were performed using 0.5 mM 2,4-DAP as the substrate in 50 mM
428 acetate (filled circles), 50 mM KPB (open squares), HEPES-NaOH (filled triangles), and
429 CHES-NaOH (filled diamonds) as described in the Materials and Methods. Error bars represent the
430 standard deviation of three independent experiments.

431

432 Figure 3. Effect of temperature on the activity of 2,4-DAPDH. Enzyme assays were performed using
433 0.5 mM 2,4-DAP as the substrate in 50 mM HEPES-NaOH (pH 8.5) at different temperatures as
434 described in the Materials and Methods. Error bars represent the standard deviation of three
435 independent experiments.

436

437 Figure 4. Substrate inhibition of 2,4-DAPDH by 2,4-DAP. 2,4-DAPDH activity is plotted as a function
438 of 2,4-DAP concentration. The solid line is a fit to the data (filled circles) according to Equation 1 in
439 the Materials and Methods.

440

441 Figure 5. Activity of 2,4-DAPDH toward 2,5-DAH. 2,4-DAPDH activity was plotted as a function of
442 2,5-DAH concentration. The solid line is a fit to the data (filled diamonds) according to the
443 Michaelis-Menten equation.

444

445 Figure 6. Inhibition of 2,4-DAPDH by D-ornithine. Double-reciprocal plots were generated at the
446 following D-ornithine concentrations: 0 mM (filled diamonds), 0.5 mM (open circles), 1.5 mM (filled
447 triangles), and 2.0 mM (open squares).
448

5. Figure 1

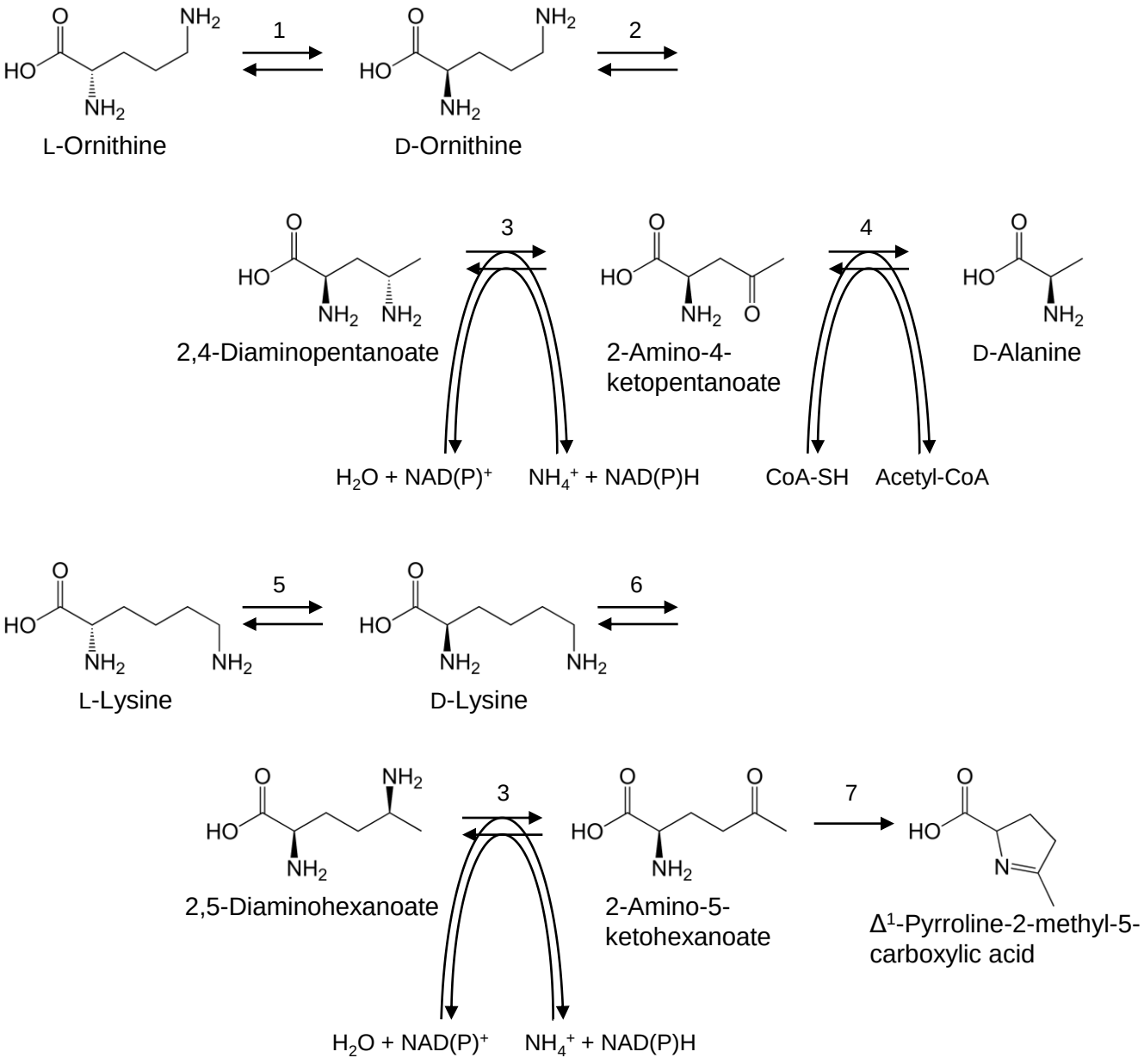

Figure 1

5. Figure 2

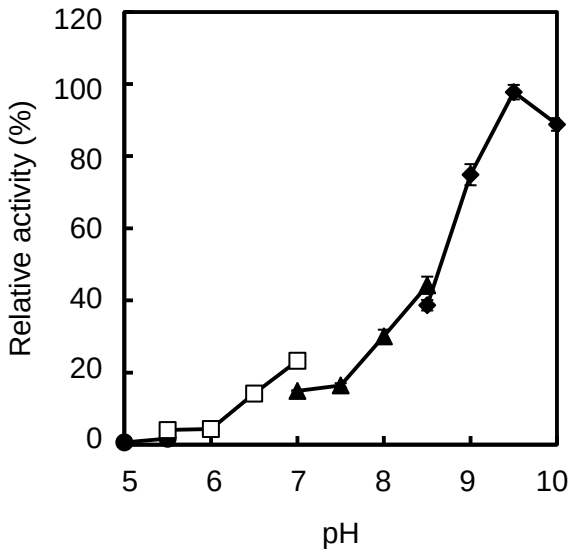

Figure 2

5. Figure 3

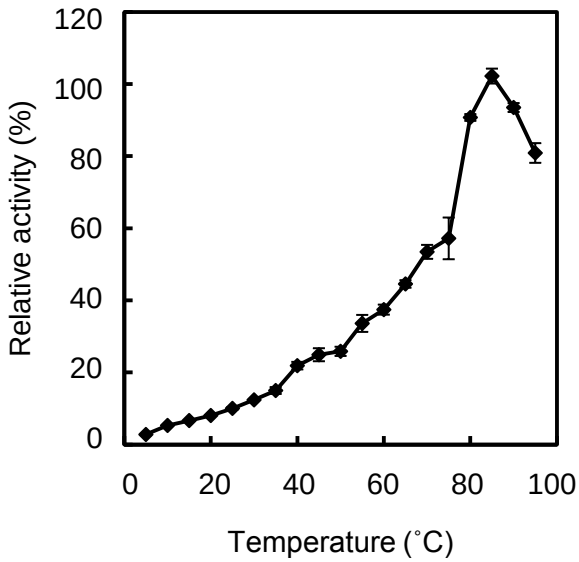

Figure 3

5. Figure 4

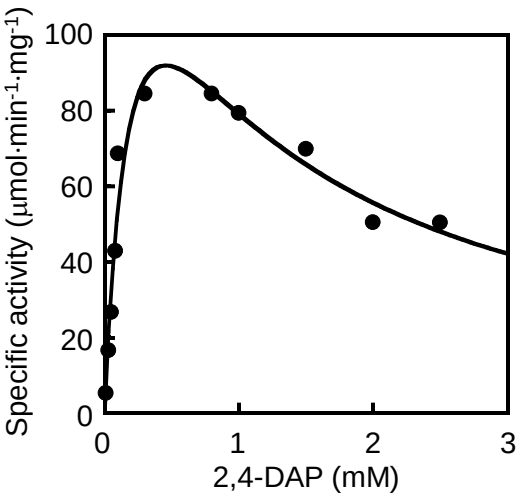

Figure 4

5. Figure 5

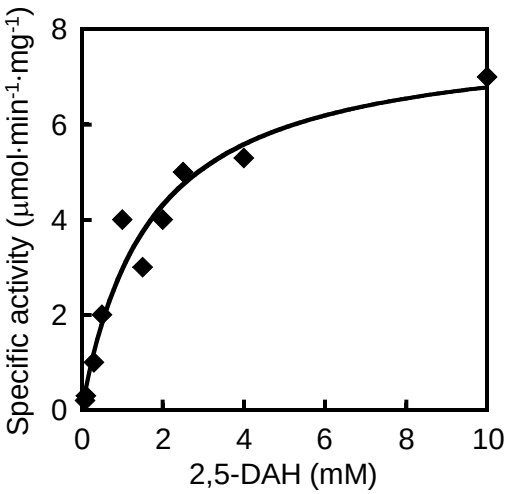

Figure 5

5. Figure 6

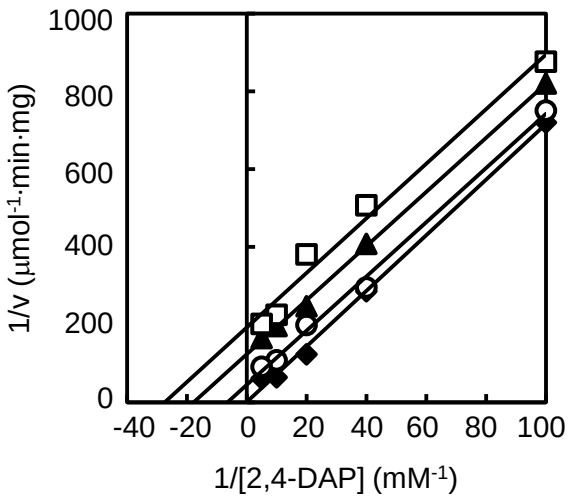

Figure 6

Table 1. Effects of various reagents on the activity of 2,4-DAPDH

	Relative activity (%)[a]
None	100 ± 0
EDTA	98 ± 6
$MgSO_4$	65 ± 11
$CaCl_2$	85 ± 7
$FeCl_2$	84 ± 4
$MnCl_2$	104 ± 0
$CoSO_4$	34 ± 4
$NiSO_4$	2 ± 1
$CuSO_4$	0 ± 0
$ZnSO_4$	2 ± 2
KCl	97 ± 4
KBr	97 ± 5
KNO_3	93 ± 2
CH_3COOK	96 ± 4
K_2SO_4	96 ± 5

[a] The values are shown as the mean ± standard deviation of three independent experiments.

Table 2. Kinetic parameters of 2,4-DAPDH

	K_m (mM)	K_i (mM)	V_{max} ($\mu mol \cdot min^{-1} \cdot mg^{-1}$)	k_{cat} (s^{-1})	k_{cat}/K_m ($mM^{-1} \cdot s^{-1}$)
NAD^+	0.05	-	97	65	1,300
$NADP^+$	2	-	86	57	29
2,4-DAP	0.2	0.9	180	65	330
2,5-DAH	2	-	0.9	0.0006	0.0003